Genomics of Neotropical biodiversity indicators: two butterfly radiations with rampant chromosomal rearrangements and hybridisation

Eva SM van der Heijden[1,2], Karin Näsvall[1], Fernando A. Seixas[3], Carlos Eduardo Beserra Nobre[4], Artur Campos D Maia[4,5], Patricio Salazar-Carrión[1,2], Jonah M Walker[1,2], Daiane Szczerbowski[6], Stefan Schulz[6], Ian A Warren[2], Kimberly Gabriela Gavilanes Córdova[7], María José Sánchez-Carvajal[7], Franz Chandi[7], Alex P Arias-Cruz[7], Nicol Rueda-M[1,8], Camilo Salazar[8], Kanchon K Dasmahapatra[9], Stephen H Montgomery[10], Melanie McClure[11], Dominic E Absolon[1], Thomas C Mathers[1], Camilla A Santos[1], Shane McCarthy[1], Jonathan MD Wood[1], Gerardo Lamas[12], Caroline Bacquet[7,13], André Victor Lucci Freitas[14], Keith R. Willmott[15], Chris D Jiggins[2], Marianne Elias[13,16], Joana I Meier[1,2]

1. Tree of Life Programme, Wellcome Sanger Institute, UK
2. Department of Zoology, University of Cambridge, UK
3. Department of Organismic and Evolutionary Biology, Harvard University, Cambridge, MA, USA
4. Graduate Program in Animal Biology, Federal University of Pernambuco, Brazil
5. Graduate Program in Plant Biology, Federal University of Pernambuco, Brazil
6. Institute of Organic Chemistry, Technische Universität Braunschweig, Germany
7. Universidad Regional Amazónica Ikiam, Ecuador
8. Biology Program, Faculty of Natural Sciences, Universidad del Rosario, Bogotá, Colombia
9. Department of Biology, University of York, UK
10. University of Bristol, UK
11. Laboratoire Écologie, Évolution, Interactions des Systèmes Amazoniens (LEEISA), Université de Guyane, CNRS, IFREMER, Cayenne, France
12. Museo de Historia Natural, Universidad Nacional Mayor de San Marcos, Lima, Peru
13. Smithsonian Tropical Research Institute, Gamboa, Panama
14. Universidade Estadual de Campinas, Brazil
15. Florida Museum of Natural History, USA
16. Institut de Systématique Évolution Biodiversité (ISYEB), CNRS, MNHN, EPHE, Sorbonne Université, Université des Antilles, Paris, France

Author contributions:

PSC, JIM, ESMH, KGGC, MJSC, DS, FC, APAC, CB, NRM, CS, KKD, NN, SHM, MM, KRW, AVLF, CDJ and ME collected samples. GL, KRW and ME oversaw the butterfly identification and taxonomic revision. ESMH, JIM, JMW and IAW performed lab work. ESMH mapped and filtered the sequencing data, and ran the phylogenetic and hybridisation analyses. KN did the chromosomal rearrangement analysis. CEBN, ACDM, DS, SS and AVLF analysed the androconial semiochemicals. FAS ran the MSCi analysis. DEA, TCM, CAS, SM, KN and JW assembled and curated the new genomes. JIM designed the study with contributions from ESMH, ME and CDJ. ESMH, JIM and KN wrote the manuscript with contributions from all authors.

Corresponding author: Joana Isabel Meier, joana.meier@sanger.ac.uk

Key words: Speciation, biodiversity, butterflies, neotropics, genomics

Classification: Biological Sciences - Evolution

Abstract

A major question in evolutionary biology is what drives the diversification of lineages. Rapid, recent radiations are ideal systems for addressing how new species arise because they still show key morphological and ecological adaptations associated with speciation. While most studied recent radiations have evolved in an insular environment, less research has been carried out on continental radiations with complex species interactions. *Melinaea* and *Mechanitis* butterflies (Nymphalidae: Ithomiini) have rapidly radiated in the Neotropics. They are classical models for Amazonian biogeography and colour pattern mimicry and have been proposed as biodiversity indicators. We generated reference genomes for five species of each genus, and whole-genome resequencing data of most species and subspecies covering a wide geographic range to assess phylogeographic relationships, patterns of hybridisation and chromosomal rearrangements. Our data help resolve the classification of these taxonomically challenging butterflies and reveal very high diversification rates. We find rampant evidence of historical hybridisation and putative hybrid species in both radiations, which may have facilitated their rapid diversification. Moreover, dozens of chromosomal fusions and fissions were identified between congeneric species, and even some within species. We conclude that interactions between geography, hybridisation and chromosomal rearrangements have contributed to these two rapid radiations in the highly diverse Neotropical region. We suggest that rapid radiations may be spurred by repeated periods of geographic isolation during Pleistocene climate oscillations, combined with lineage-specific rapid accumulation of incompatibilities during allopatric phases, followed by secondary contact with some gene exchange.

Significance Statement

Understanding factors contributing to rapid speciation is a key aim of evolutionary biology. Here we focus on two rapid radiations of Neotropical butterflies. Our genomic data with broad taxonomic and geographic coverage reveal rampant hybridisation and chromosomal rearrangements, each likely contributing to the high diversification rates. Our study highlights the use of genomic data to resolve taxonomically challenging species groups and elucidate drivers of diversification in rapid radiations. We show that for biodiversity hotspots with recent radiations, barcoding is insufficient to characterise species richness due to gene flow and recent speciation. The taxonomic implications of both introgression and karyotype diversity for species delimitation are important to consider during monitoring and management of biodiversity in these vulnerable habitats.

Introduction

Rapid radiations, where a lineage diversifies into many different species over a short time period, are ideal systems for studying how new species evolve (1, 2). They can be driven both by non-adaptive processes, such as the accumulation of differences during periods of allopatry leading to incompatibilities upon secondary contact, and by adaptive processes such as adaptation to different ecological niches or sexual selection for different traits and preferences (3, 4). Sympatric radiations require some degree of niche differentiation among the species for stable coexistence and sufficient reproductive isolation such that incipient lineages do not merge (2).

While most lineages do not readily radiate even in the face of ecological opportunity, some lineages are particularly prone to rapid radiations, and do so repeatedly. We are only starting to understand the factors explaining these lineage-specific differences (5). Most knowledge stems from well-studied radiations that evolved in insular environments with little competition with other species and a relatively simple and geographically limited environment (e.g. Darwin's finches on the Galapagos Islands, cichlid fishes in lakes, *Anolis* lizards on the Caribbean islands or Hawaiian silverswords) (2, 6). However, many rapid radiations evolved on the much more complex continents and much less is known about drivers leading to their diversification (7–9). Reduced competition in insular environments allows niche specialisation without being immediately outcompeted when a lineage is not yet well-adapted to its environment. However, in large continental areas such as the hyperdiverse Neotropics, competition is much stronger limiting ecological speciation. On the other hand, large and complex environments on continents may provide more opportunity for allopatric divergence than a small island. The speed of accumulating incompatibilities in allopatry may thus be more important in rapid radiations on continents than insular environments.

Here, we study the drivers of diversification in two rapid continental radiations of the Neotropical butterfly tribe Ithomiini. Ithomiine butterflies (Nymphalidae: Danainae, ca. 400 species in 42 genera) are found across Central and South America (10, 11). They constitute a substantial part of the butterfly species assemblage and are regarded as good indicators of spatial patterns of biodiversity in the Neotropics, the most biodiverse areas in the world (10, 12, 13). Sequestration of pyrrolizidine alkaloids from Asteraceae and Boraginaceae plants render most Ithomiini unpalatable (14–18), and their colour patterns advertise this unpalatability to predators. They form Müllerian mimicry rings, where locally co-occurring species have converged in colour pattern, and thus share the cost of educating predators (10, 19, 20). We focus on two ithomiine genera, *Melinaea* and *Mechanitis*, which have diversified exceptionally fast with most species younger than a million years (11, 21). Hitherto, the study of these radiations has been hampered

by taxonomic challenges. *Melinaea* and *Mechanitis* are among the most taxonomically difficult of Ithomiini, as Fox noted (1967) (22): 'these insects [are] so thoroughly confusing and so thoroughly confused by my predecessors'. The species do not differ in genital or other morphological characteristics and show substantial intraspecific wing pattern variation and mimicry between taxa. Barcoding does not reliably distinguish species either (23, 24). As prior studies have only used few or no genetic markers or did not have broad geographic coverage, the taxonomy is still partially unresolved, despite many taxonomic revisions (22, 24–26, e.g. 27–29).

While the exact causes of their rapid radiations are unknown, different contributing factors have been proposed. Ecological adaptation may be relevant as species show differences in microhabitats, host plants, mimicry rings, and altitude, but on the other hand many species share habitats and host plants, and the majority of species occurs in the lowlands (25, 30–33). Moreover, where species co-exist, they converge in colour patterns and thus assortative mating may rely more strongly on chemical cues. Ithomiine species differ in male-specific androconial compounds (chemical compounds secreted from specialised wing scales where the fore- and hindwing overlap), which likely act as pheromones (Trigo et al. 1996; Schulz et al. 2004; Blow et al. 2023).

Allopatric accumulation of differences could also have played a role in the rapid diversification of ithomiini, as this could have occurred in different rainforest refugia during climatic oscillations e.g. in the Pleistocene (26, 34, but see 35, 36) or on opposite sides of geographic barriers such as the Andes. Both climatic refugia and the Andes have been proposed as "speciation pumps" in the Neotropics (37), also for Ithomiini (38), where periods of allopatry followed by secondary contact create favourable circumstances for speciation.

Another factor that might contribute to the diversification of ithomiine butterflies is hybridisation. Phylogenetic studies using a limited number of markers have revealed mito-nuclear discordances and paraphyletic taxa in Ithomiini (23, 36). This could be due to limited geographic or genetic resolution, incomplete lineage sorting in the rapidly speciating lineages, or introgressive hybridisation. While gene flow between sister lineages can homogenise their gene pools, opposing speciation, recent studies have shown that sometimes introgressive hybridisation from more distant relatives can facilitate rapid diversification by enriching the genetic diversity with novel, potentially adaptive variants or contributing to the origin of new hybrid species (39–43). Admixture has been shown to kickstart adaptive radiation (e.g. 44, 45), facilitate parallel adaptation (e.g. 42, 46), and novel adaptations (e.g. 47), but the role in ithomiini diversification is hitherto unknown.

Ithomiini butterflies have an unusually high diversity in chromosome number (48), which could also contribute to their rapid diversification. Offspring from parents with different karyotypes may suffer reduced fitness, due to mismatch in pairing of homologous chromosomes that results in aneuploidy, meiotic failure or hybrid sterility (49, 50). Furthermore, chromosomal rearrangements might facilitate divergence in the face of gene flow by accumulation of incompatibilities in low recombining regions (51) or if they link together co-adapted variants (52, 53). In *Melinaea* and *Mechanitis* butterflies, chromosome counts range from 13 to 30 (48), and chromosomal rearrangements likely contribute to reproductive isolation, as a cross between two closely-related *Melinaea* species with different karyotypes resulted in nearly sterile hybrids (54). However, pervasive intraspecific variation in chromosome counts (48, 54) indicates that not all rearrangements reduce fitness and their role in speciation thus remains an open question.

Here, we use five reference genomes of each genus and whole-genome resequencing data of almost all species and many subspecies, to resolve taxonomic uncertainties and explore whether geography, introgressive hybridisation or chromosomal rearrangements may have played a role in the rapid diversification of *Mechanitis* and *Melinaea* butterflies.

Results

Taxonomic revision

In this manuscript, we adhere to the 'genotypic cluster' species concept, which defines a species as 'a morphologically or genetically distinguishable group of individuals that has few or no intermediates when in contact with other such clusters' (55). Through whole-genome resequencing of 135 *Mechanitis* and 109 *Melinaea* individuals from across South and Central America, with additional individuals from the outgroup genera *Forbestra*, *Eutresis* and *Olyras*, we shed light on the phylogenomic relationships and taxonomy (Fig. 1). Our results, laid out in the following sections (see also Text S1), confirm species versus subspecies status for most known taxa in agreement with (29), support two recent species reclassifications (*Mel. tarapotensis* (54), *Mel. mothone* (56)) and reveal three additional taxa that need to be elevated to species level (*Mel. maeonis* **stat rest** (Hewitson 1869), *Mec. nesaea* **stat rest** (Hübner 1820), *Mec. macrinus* **stat rest** (Hewitson 1860), Fig. 1; Text S1). The placement of *Mel. menophilus mediatrix* (French Guiana) has been uncertain (56); our dataset places it as the most divergent subspecies of *Mel. menophilus*. A revised, annotated taxonomic list for these two genera can be found in Text S2.

Mitonuclear discordance

In both *Mechanitis* and *Melinaea*, we find rampant mitonuclear discordance, *i.e.* mismatches between mitochondrial and nuclear phylogenies (IQtree2; maximum likelihood) (Fig. 1). For instance, *Mec. nesaea* is sister to *Mec. polymnia* in the nuclear phylogeny, but to *Mec. lysimnia* in the mitochondrial phylogeny (Fig. 1A - box III; Fig. S1-2). This result could either be indicative of incomplete lineage sorting (ILS) or admixture (more details below). *Mec. messenoides* harbours two divergent mitochondrial haplotypes, consistent with barcoding results (23, 25) (Fig. 1A - box II), one clustering with the *polymnia-lysimnia* clade, and the other one with its nuclear sister species, *Mec. menapis*. The mitochondrially divergent *Mec. messenoides* individuals do not form separate clades in the nuclear phylogeny, nor do they differ in collection location or subspecies (Table S1; Fig. S1-2).

While the *Melinaea* species are clearly differentiated in the nuclear phylogeny, the mitochondrial phylogeny shows almost no variation among species, confirming previous barcoding results (56) (Fig. 1B; Fig. S3-4). *Mel. ludovica*, *Mel. tarapotensis* and *Mel. lilis* are the only species that form monophyletic mitochondrial clades that are no part of the shallow clade without species differentiation. Notably, *Mel. ludovica* is the only species that is also an outgroup to the other *Melinaea* species in the nuclear genome, whereas *Mel. lilis* and *Mel. tarapotensis* are sister to *Mel. isocomma* and *Mel. satevis*, respectively.

Calibrated phylogenetic tree

We approximated the divergence times in the two genera using a Bayesian multispecies coalescent method for inferring species trees (StarBEAST2), with one individual representing each lineage to produce a phylogeny calibrated with divergence times from (11) (Fig. 2). The seven *Mechanitis* species are estimated to have diversified within the past 1.36 million years, resulting in a speciation rate of 1.431 speciation events per lineage/My (assuming a pure birth model with a constant speciation rate). The ten species of the core *Melinaea* clade (excluding the most divergent species, *Mel. ludovica*) have diversified in the past 1.41 million years (Fig. 2B), giving a speciation rate of at least 1.633. Of the four potential *Melinaea* species missing in our analysis (*Mel. ethra*, *mnasias, mnemopsis* and *scylax*), two likely form part of the core clade (11, 57), which would increase the speciation rate to 1.672.

However, note that gene flow could affect our estimates, as suggested by discordance between the StarBEAST2 and IQtree2 topologies (Fig. 2 vs Fig. 1 (note low concordance factors in Fig. 1)): *Mec. messenoides* is not sister to *Mec. menapis* anymore, and *Mec. nesaea* has shifted to be sister to *Mec. lysimnia* instead of *Mec. polymnia*. The relationships among lineages within *Mec. polymnia* also changed. While ILS could partially explain this, introgression could also cause it (see details below). Gene flow

between sister lineages will make their apparent divergence times shorter than the initial split time, and gene flow with non-sister lineages will make them appear longer.

Phylogeographic patterns

Through combining our sampling locations with those compiled by (10) adjusted according to our taxonomic revision (Fig. 2), we assessed the biogeographic distribution of the species. We find four main biogeographic regions (Fig. 2; Fig. S6-7), with most species restricted to one of them. Some sister-species are separated by the Andes: *Mec. messenoides* and *mazaeus* (Western Amazonia) versus their respective sisters *Mec. menapis* and *macrinus* (West of the Andes). However, note that the placement of *Mec. messenoides* differs in the StarBEAST2-topology and is affected by hybridisation (see next section). Within *Mec. polymnia*, Ecuadorian and Colombian individuals from opposite sides of the Andes are highly divergent, indicating little gene flow, though our study includes one putative hybrid (Fig. S8). This pattern of species separation by the Andes was not previously as apparent due to species misclassification.

Most individuals in our *Melinaea* dataset are from Western Amazonia (east of the Andes) and we find that many sister species are sympatric. Only two species in our dataset occur west of the Andes (*Mel. lilis* and *idae*) and they form a clade with a third species from east of the Andes (*Mel. isocomma*). Our dataset lacks a potential third species occurring west of the Andes, *Mel. scylax* (10), which may represent a subspecies of *Mel. lilis* (26, 57). Other potential species missing in our dataset are *Mel. mnemopsis* from Western Amazonia, *Mel. ethra* from the Atlantic forest and *Mel. mnasias* from Western Amazonia and the Atlantic Forest (10, 57).

Signatures of rampant introgression throughout both genera

Phylogenetic discordance between phylogenies constructed for the nuclear and mitochondrial genome (Fig. 1), for different genomic regions inferred with concordance factors (Fig. 1), and with IQtree2 and StarBEAST2 (Fig. 1 vs Fig. 2) is indicative of a history of introgression and/or ILS in both genera. We assessed hybridisation throughout both radiations with windowed species tree inference with BPP (Fig. S5), excess allele sharing between non-sister taxa estimated from Fbranch (Fig. S9) and joint inference of species tree with gene flow using the approximate isolation with migration (AIM) model (Fig. S10). The resulting phylogenies and introgression histories are summarised in Fig. 2 (Text S3), but we stress that this is only one of multiple possible scenarios consistent with our observed patterns of excess allele sharing and gene tree discordance.

In *Mechanitis*, two lineages show uncertain placements. As mentioned, the placement of *Mec. messenoides* and *nesaea* varies depending on the methodology (IQtree2 and StarBEAST2) and genomic regions (Fig. 1A – box II and III). Contrary to the nuclear phylogeny inferred with StarBEAST2, but in line with the mitochondrial phylogeny, the species phylogeny inferred allowing for gene flow (AIM) places *messenoides* closer to the *polymnia-nesaea-lysimnia* clade rather than with *menapis-mazaeus-macrinus*. AIM indicates admixture between these clades (Fig S10A – arrows B-D), and Fbranch also confirms excess allele sharing between *messenoides* and *polymnia-nesaea-lysimnia* (Fig. S9A - #1). According to the BPP-analysis, *Mec. messenoides* groups with menapis-mazaeus-macrinus in ~51% of the genome, and with *polymnia-lysimnia-nesaea* in ~28% of the genome (sometimes still with *Mec. menapis*) (Fig. 5B). The branching order within the *polymnia-lysimnia-nesaea* clade is also highly variable across the genome: *polymnia* and nesaea are sister in 46.3% of the genome grouping, while 31.7% of trees group *polymnia* with *lysimnia*, and 14.7% group *nesaea* with *lysimnia* (Fig. 5C) (see also Fbranch - Fig. S9A #3). In short, these results are consistent with *Mec. messenoides* being introgressed (Fig 2A - arrows a-d) and gene flow between *polymnia-lysimnia-nesaea*.

In *Melinaea*, IQtree2 and StarBEAST2 produce the same topology (Fig. 1 vs Fig. 2), with *Mel. idae* sister to *Mel. lilis* and *Mel. isocomma*. However, the AIM analysis groups *Mel. idae* with the ingroup clade, although showing extensive gene flow from the lineage of *Mel. lilis* and *Mel. isocomma* (Fig. 2B - arrow a; Fig S10B – arrow A,D; see also Fbranch (Fig. S9B - #1)). To resolve the position of *Mel. idae*, as well as putative introgression between deeper branches of the phylogeny, we ran BPP focusing on the relationships between the *lilis-isocomma-idae* clade and representatives of the ingroup clade (*mneme*, *marsaeus* and *mothone*) (Fig. 5E-F). In the majority of the genome (43.4%) *lilis, idae* and *isocomma* group together (like IQTree2 and StarBEAST2), while in 34.5% of the genome *idae* groups with *mothone-marsaeus-mneme* (like AIM). Notably, the Z chromosome supports almost exclusively the latter relationship. In 4.3% of the genome, *isocomma* clusters with *mothone-marsaeus-mneme*. *Mel. lilis* is almost as often sister to *idae* (30.3%) as to *isocomma* (38.3%), and less commonly an outgroup to both (4.1%), indicating more recent shared ancestry between *lilis* and *idae*, which is confirmed by Fbranch excess allele sharing (Fig. S10B; Fig S9B - #2). *Mel. mothone, marsaeus* and *mneme* also vary in their respective relationships (Fig. 5E).

We further investigated the timing of divergence and introgression for the three species showing the strongest signals of introgression (*Mec. messenoides*, *Mec. nesaea* and *Mel. idae*), using a multispecies coalescent-with-introgression (MSCi) approach. In all three cases, introgression is estimated to be old (200-425 kya) (Fig. 3A-B scenario 1; Fig. 3C). For *Mec. messenoides* and *Mel. idae,* different replicate runs

262 produce different outcomes reflecting the uncertainty in the placement of these two species in the
263 phylogeny. Notably, some replicates indicate the origin of the introgressed lineages closely coincides with
264 the split time from both parents, suggestive of a hybrid origin (Fig. 3A-B scenario 2; Fig. S11; Table S2).
265

266 **A focus on *Mec. nesaea***

267 As we propose to re-elevate *Mec. nesaea* to a species from its previous classification as a subspecies of
268 *Mec. lysimnia*, we investigated the relationships and reproductive isolation between *Mec. nesaea*, *Mec.*
269 *lysimnia* and *Mec. polymnia* in more detail. We resequenced 15 *Mec. nesaea*, 19 *Mec. l. lysimnia* and 9
270 *Mec. p. casabranca*, of which 24 were sampled from sympatry, and assessed the androconial compounds
271 that might act as pheromones, potentially contributing to assortative mating. Even though *Mec. lysimnia*
272 and *Mec. polymnia* have been observed to interbreed in nature (58) and putative hybrids have been
273 observed (Fig. S12), we find relatively high F_{ST} throughout the genome between all three species and no
274 evidence of ongoing gene flow based on ADMIXTURE analyses (Fig. S8; S13). Furthermore, they have been
275 shown to differ in number of chromosomes (Fig. 3D) (48), and we find their androconial bouquets to be
276 clearly distinct (Fig. 3E-F, Text S4; Table S3-4). All these lines of evidence suggest strong reproductive
277 isolation between *Mec. nesaea* and both *Mec. polymnia* and *Mec. lysimnia.* Genome scans for
278 introgression (f_{dM}) between *Mec. lysimnia* and *Mec. nesaea* compared to allopatric *Mec. polymnia* show
279 that this introgression is restricted to few genomic regions (Fig. 3G; Fig. S14-S15). The MSCi model for
280 *Mec. nesaea* suggests *Mec. nesaea* diverged from *Mec. polymnia* prior to *Mec. lysimnia* introgression.
281 However, *lysimnia*-introgression could have contributed key genetic variation to *Mec. nesaea* and
282 strengthened reproductive isolation to *Mec. polymnia*. Consistent with this hypothesis, we find that
283 introgression peaks coincide with peaks of elevated D_{xy} and F_{ST} between *Mec. nesaea* and *Mec. polymnia*
284 and mostly show no evidence of excess allele sharing between *Mec. nesaea* and sympatric *Mec. polymnia*
285 compared to allopatric *Mec. polymnia* (Fig. 3G; Fig. S13-S15), but the low levels of ongoing gene flow make
286 these measures poor predictors of reproductive isolation barriers.
287

288 **Chromosomal rearrangements**

289 To study chromosomal rearrangements, we generated haplotype-resolved genomes of five *Melinaea* and
290 five *Mechanitis* species using PacBio and HiC-data (Fig. S16), resulting in high quality genomes with >96%
291 BUSCO completeness and >94% of the genome assembled to chromosomes (Table S5-S6). The inferred
292 chromosome numbers match the chromosome counts from karyotyping (48). The *Mechanitis* genomes
293 are substantially shorter (291-320 Mb) than the *Melinaea* genomes (496-661 Mb, Table S5).

Whereas most Lepidoptera have conserved karyotypes with 31 chromosomes (59), our synteny analysis using BUSCO genes show that *Mechanitis* and *Melinaea* genomes are highly rearranged compared to the ancestral karyotype (Fig. S17-S19), corroborating earlier findings from two *Melinaea* genomes (60). The median length of conserved syntenic blocks is 32-36 genes, compared to 168 genes in the outgroup *Danaus plexippus* (Table S7; Fig. S19). The canonical Z has not undergone any fissions and has retained the longest conserved syntenic blocks (225-227 genes; Fig. 4A; Table S7; Fig. S19) in our genomes. However, both genera share a fusion of Z with parts of ancestral autosome 10 and *Mechanitis* has a further fusion with parts of ancestral autosome 6 (Table S8; Fig. S18). In addition, a fusion-fission polymorphism involving the Z and another autosome was observed between the Zs of the male *Mel. isocomma* (Table S8; Fig. S16). A W-chromosome was identified in all females as a segment of varying size depleted of BUSCO genes with moderate sequence similarity within genera, but none between (Fig. 4A). We found W-autosome fusions in four species (Table S8). *Mec. macrinus* and *mazaeus* show complex fusions between the W and multiple autosomes that are partially shared. Four species have two Z chromosomes, as by definition, the homologue of the chromosome fused to the W becomes a Z chromosome. Similarly, three species have two or three W chromosomes. Surprisingly, seven individuals were heterozygous for one or more simple autosomal rearrangement and in *Mel. ludovica* we detected a complex chain rearrangement involving four autosomes in one haplotype and three autosomes in the other haplotype (Table S8; Fig. S16). None of the simple autosomal polymorphisms are shared among taxa.

While chromosome spreads had revealed species differences in chromosome counts (48), we here show that these are not due to a few fissions or fusions, but complex rearrangements. Closely related sister species show 3-47 chromosomal rearrangements (Fig. 4), which could contribute to reproductive isolation. To assess if these chromosomal rearrangements confer reproductive isolation barriers, we mapped the location of the chromosomal breakpoints between all species pairs to test for an association between breakpoints and reduced gene flow. We found increased F_{ST} in all *Mechanitis* comparisons, and reduced diversity (π) in breakpoint regions in seven of the ten comparisons (Fig. 4B, Fig. S20, Table S9). In principle, elevated F_{ST} could be caused by increased background selection as recombination tends to be reduced at chromosome ends and levels of ongoing gene flow are low (61, 62). However, we also find elevated absolute divergence (D_{XY}) in windows coinciding with breakpoints in four of the ten comparisons, which indicates that background selection alone cannot explain the pattern (63). In *Melinaea*, we did not observe significantly elevated F_{ST} in the breakpoint regions, but we detected an increase in D_{XY} especially in the comparisons involving the more distantly related *Mel. ludovica* (Table S9).

Discussion

Our results confirm that the two ithomiine genera *Melinaea* and *Mechanitis* represent fast and recent radiations. They diverged in the past 1-2 million years, and speciated much faster than the other well-studied Neotropical butterfly radiation of *Heliconius* (respectively 1.633 and 1.431 versus 0.324 speciation events per lineage/My (46 species in 11.8 My)) (64). Kawahara et al. (21) previously found a significant rate shift towards high diversification rates in ithomiine butterflies (clade L; 0.23 speciation events per lineage/My) and we show that among Ithomiini, *Mechanitis* and *Melinaea* have an even higher speciation rate, consistent with previous results (11). Our results shed light on potential drivers of their rapid diversification, detailed below.

Given the high number of ancient introgression events across both genera, hybridisation may have sped up speciation by boosting genetic variation as seen in other systems (e.g. 42). We identified three species showing ancient introgression that might have a hybrid origin. Further research on which genomic regions are more or less likely to introgress could inform us as to what extent introgression contributed to reproductive isolation between those taxa and their parental lineages. For instance, similar to *Heliconius* butterflies, introgression might have contributed to both mimicry ring switches and colour-based assortative mating, which generate reproductive isolation, thereby driving speciation (65).

Despite ancient hybridisation, we find little evidence for ongoing gene flow between the species, suggesting strong reproductive isolation. Some of this reproductive isolation is likely attributed to the exceptionally high rates of chromosomal rearrangements across both genera, as complex chromosomal rearrangements are expected to constitute barriers to gene flow (66, 67). While Lepidoptera chromosomes are holocentric and may be able to tolerate simple fusions and fissions during meiosis, most Lepidoptera have retained the same highly conserved karyotypes of 31 chromosomes (59, 68). The massive chromosomal rearrangements we found in ithomiini are thus unusual, but there are other lineages that also show high rates of fissions and fusions (e.g. *Leptidea* (69); and *Erebia* (70)) and there is a slight association with variation in chromosome number and speciation rates (71).

Even though chromosomal rearrangements are thought to limit gene flow, many of our genomes showed heterozygosity for chromosomal rearrangements. The heterozygote fission-fusions are unambiguous in the HiC-data, matching the intraspecific variation in chromosome counts documented previously (48) and cytogenetical evidence for pervasive polymorphism in *Mel. satevis cydon* (54). This may be akin to *Leptidea sinapis*, where, despite multiple fusion/fission polymorphisms segregating within populations (69, 72), crosses between chromosomal extremes show low survival of F2 hybrids (73). That complex chromosomal rearrangements involving multiple chromosomes likely constitute stronger

barriers to gene flow compared to simple fusions and fissions has also been found in other taxa such as shrews (74) and wallabies (75) and is in line with findings of nearly sterile hybrids in a cross between two *Melinaea* sister species that differ in chromosome count (54). It is thus possible that simple fusions and fissions are not strongly selected against, but if too many sequential fusions accumulate in isolated populations, they cause reproductive isolation upon secondary contact.

Furthermore, we find many fusions between sex chromosomes and autosomes. Given the disproportionate role sex chromosomes are proposed to have in speciation (Haldane's rule and/or large-Z effect) (76–78), they may play a strong role in reproductive isolation of ithomiini butterflies. We found two Z-autosome fusions shared among all congenerics, but no fission in the canonical Z, consistent with conserved Z chromosomes in other Lepidoptera lineages (68). The heterozygote Z-autosome fusion in *Mel. isocomma* potentially represents an ongoing fixation of a novel Z-autosome fusion, which might rapidly rise in frequency if there are advantageous loci involved (79). The simple W-autosome fusion observed in *Mel. menophilus* resemble those described in some *Heliconius* butterflies (80). The complex fusion-fissions with multiple Ws and Zs in *Mec. macrinus* and *Mec. mazaeus* are similar to *Leptidea* butterflies (81) and may constitute particularly strong barriers to gene flow (82).

Since the divergence times of *Mechanitis* and *Melinaea* species match Pleistocene climatic fluctuations (2.58 Ma-11.7 ka), and many sister species are separated by the Andes or restricted to different geographic regions corresponding to postulated Pleistocene refugia (26, 34, 37), we believe that our findings are consistent with the speciation pump hypothesis. This hypothesis postulates that periods of allopatry, followed by secondary sympatry, can facilitate diversification (37), as proposed in e.g. fishes (45, 83) and Andean plants (84). The high rates of chromosomal rearrangements in *Mechanitis* and *Melinaea* might accelerate the accumulation of chromosomal differences in isolated populations. On coming together in secondary sympatry, these rearrangements likely cause low hybrid fitness, which in turn might facilitate adaptation to different niches due to low levels of gene flow. Selection against interbreeding might also lead to reinforcement of reproductive isolation via assortative mating, e.g. based on pheromones (18, 85).

Our data suggests that hybridisation-derived genetic variation and high rates of chromosomal rearrangements both may have played key roles in the fast diversification of *Melinaea* and *Mechanitis*, and potentially contributed to adaptation and assortative mating facilitating species coexistence. Notably, while an important role of hybridisation in diversification has been found in both insular environments (e.g. silverswords (44), or cichlids (45)) and continental radiations (e.g. this study, *Heliconius* (86), or *Rhagoletis* flies (87)), rapid radiations with high rates of chromosomal rearrangements seem to be

restricted to continents (e.g. this study, shrews (74), or wallabies (75)). Due to more opportunities for geographical isolation on large land masses than in insular environments, factors such as high rates of chromosomal rearrangements that speed up the allopatric accumulation of incompatibilities may thus be particularly important in continental radiations.

Our study not only sheds light on drivers of continental radiations, but also largely resolves the taxonomy of important biodiversity indicators. Hitherto, the study of these radiations has been hampered by taxonomic challenges, whereas our combination of whole-genome resequencing with vast taxonomic and geographic coverage, genome assemblies and androconial chemical analysis allowed us to resolve taxonomic issues. Our study confirms that DNA barcoding can be misleading, massively underestimating species richness, and should only be used with care to assess biodiversity. The taxonomic implications of both introgression and karyotype diversity for species delimitation and designation of conservation units are important to consider during monitoring and management of biodiversity in these vulnerable habitats.

Materials and methods

Collecting butterfly specimens

157 specimens of *Mechanitis*, 9 specimens of *Forbestra*, 109 specimens of *Melinaea,* 1 *Eutresis* and 1 *Olyras* were collected over the years 2000 to 2023 across Central and South America (Table S1). Adult butterflies were caught with a net, and their bodies were subsequently preserved in ethanol, DMSO or flash-frozen and stored at -70°C. Moreover, a few legs from dried museum specimens were used (Florida Natural History Museum; Natural History Museum London). Wings were photographed and stored in envelopes. The resulting dataset covers almost all species of *Melinaea* and *Mechanitis* from a wide geographical range. In addition, 65 individuals of *Mec. lysimnia nesaea* (status restored to *Mec. nesaea* in this paper; hereafter called *Mec. nesaea*), 19 *Mec. lysimnia lysimnia* and 8 *Mec. polymnia casabranca* were collected for the androconial chemical analysis (Table S3).

DNA extractions & whole genome resequencing

DNA extractions were done with either the Qiagen MagAttract High Molecular Weight kit (Qiagen ID 67563), or the Qiagen QiaAmp DNA mini kit (51304), or a PureLink digestion and lysis step followed by a magnetic bead DNA extraction (88). The dried museum specimens were extracted using a Lysis-C buffer and a MinElute DNA extraction kit (protocol adapted from (89); Qiagen ID 28006). Library preparations were performed using homemade TN5-transposase-mediated tagmentation (protocol adapted from (90)), or following the manufacturer's guidelines with the Illumina DNA PCR-free library prep kit and

422 sequenced (150 bp paired-end) on Illumina NovaSeq 6000 or NovaSeq X machines at Novogene or the
423 Wellcome Sanger Institute.
424
425 *Reference genomes*
426 Haplotype-level chromosomally resolved reference genomes were assembled for five species of
427 *Mechanitis* (*Mec. messenoides, menapis, mazaeus, macrinus* and *polymnia*) and *Melinaea* (*Mel. ludovica,*
428 *marsaeus, mothone, isocomma* and *menophilus*). Note that earlier versions of two *Melinaea* genomes
429 were published previously (60). In short, we combined 12-57x PacBio HiFi sequencing and 33-197x
430 Illumina sequencing of HiC libraries (haploid coverages, Table S5) and assembled the genomes according
431 to the Tree of Life pipelines (https://github.com/sanger-tol/genomeassembly) (Text S5).
432
433 *Whole genome mapping*
434 To prepare the whole genome data for analysis, read quality was checked with FastQC (v0.11.9) (91).
435 Sequences below 50 bp were discarded and adapters and PolyG-tails were trimmed with FastP (v0.23.2)
436 (92), before they were aligned to *Melinaea marsaeus* (60) or *Mechanitis messenoides* using BWA-mem
437 (v.0.7.17) (93). Picard was used to remove PCR duplicates (v3.0.0) (94). Samtools (v1.17) (95) and GATK3
438 HaplotypeCaller (v3.8.1.0) (96, 97) were used for variant calling, with a minimum base quality score of 20.
439 VCFtools (v0.1.16) (98) was used for filtering. Based on the distribution of sequencing depth
440 (mean *Melinaea*: 7; *Mechanitis*: 15), all sites with a mean depth below 3 (*Melinaea*) or 5 (*Mechanitis*), and
441 above 15 (*Melinaea*) or 30 (*Mechanitis*) were removed. Insertions, deletions, sites with >50% missing data,
442 as well as genotypes with a depth below 2 (*Melinaea*) or 3 (*Mechanitis*) were removed. The mitochondrial
443 DNA was filtered separately, with a maximum depth of 1700 (*Melinaea*) or 1200 (*Mechanitis*).
444
445 *Phylogenetic analyses*
446 For each genus, we ran a Principal Component Analysis (PCA) using Plink (V1.9) to explore population
447 structure (99) (Fig. S21). Next, we inferred a phylogenetic tree based on a filtered subset of the whole
448 genome sequence data (also including monomorphic sites, thinned to 1 in 500 sites, with a minimum
449 genotype quality of 10). Our filtered VCF-files were converted to phylip with a custom script which calls
450 heterozygous sites as 'ambiguous' (equal likelihood for both alleles) to generate one sequence per
451 individual (vcf2phylip.py, http://www.github.com/joanam/scripts), and subsequently, IQtree2 (v2.1.2)
452 (100) produced phylogenetic trees with ultrafast bootstrap approximation (-B 1000; UFBoost) (101) and
453 the GTR-model.

We inferred separate phylogenies for mitochondrial and nuclear DNA. The nuclear trees are based on 537,500 SNPs for *Mechanitis* and 784,526 SNPs for *Melinaea*. The mitochondrial phylogenies are based on the full mitochondrial genome (not thinned) including 11,818 bp for *Mechanitis* and 11,815 bp for *Melinaea.* For *Mechanitis*, we included a maximum of six individuals of the same subspecies and country in the phylogenetic analyses, thus excluding several Brazilian *Mec. polymnia*, *Mec. nesaea* and *Mec. lysimnia*. These individuals were included in hybridisation-analyses. For *Melinaea*, all individuals were used.

In addition, a phylogenetic tree calibrated with divergence times from (11) was produced using StarBEAST2 (102) (following https://beast2-dev.github.io/beast-docs/beast2/DivergenceDating/DivergenceDatingTutorial.html) for the same dataset as the nuclear phylogenetic tree, but thinned further to 1 in 5000 sites and with only one individual per lineage. Divergence times between *Mec. mazaeus* and *Mec. macrinus* (0.39 MYA) and *Mel. isocomma* and *Mel. lilis* (0.65 MY) were used for calibration. We used the HKY gamma-4 site model with a strict molecular clock and the Calibrated Yule model. The model was run for 15.000.000 chains, stored every 5000 trees.

Phylogenies were visualised using the packages 'ape' (v5.7-1) and 'phytools' (v2.1-1) in R (Paradis and Schliep 2019; Revell 2024) and FigTree (v1.1.4) (http://tree.bio.ed.ac.uk/software/figtree/). To calculate a constant speciation rate (λ) we assumed a pure birth model, with n as the number of species and T the time from root to tip: $n = e^{\lambda * T}$ which gives $\lambda = ln(n)/T$.

Distribution maps

The coordinates of our individuals and the individuals from (10) were plotted using the libraries 'sf', 'tmap', 'tmaptools' and 'mapview' in R (103–105). We classified the subspecies of (10) into species following our taxonomic revision. Our individuals were plotted as dots on top of the overall distribution combining data with (10). The basemap 'Esri.WorldTerrain' was used, provided through 'Leaflet' (ESRI, ARCGIS; https://github.com/leaflet-extras/leaflet-providers); Fig. S6-7 has maps including the attribution.

Window trees

IQtree2 was used to produce phylogenetic trees in windows across the genome (one 20kb window every 200kb) and to calculate gene concordance factors between these window-trees and the whole-genome phylogenetic tree (106).

DSuite analysis

We explored excess allele sharing between species or divergent subspecies using DSuite (107). We filtered our genomic dataset to be 1 in 100 sites, only including variable sites. Dtrios calculated D and f4-ratio statistics for all trios and Fbranch then summarised them as f-branch statistics using a species tree based on the nuclear phylogeny of Fig. 2 (Table S1). The results of this analysis were visualised with a python script provided by DSuite.

AIM with StarBEAST2

We followed the Approximate Isolatoin with Migration (AIM) in StarBEAST2 tutorial to obtain a phylogenetic tree with admixture arrows (108, 109). For each genus, we picked one individual per species (highest depth), and randomly extracted 150 (*Mechanitis*) or 200 (*Melinaea*) 800-1000bp windows across the genome. We used the HKY gamma-4 site model with a strict molecular clock and the Yule model. The migration rate was set to 25 with an initial value of 0.1, and we ran the model for 100.000.000 chains, storing every 5000 trees. We updated the parameters according to the suggestions in the output of the first run and re-ran the model to improve the results.

Species-tree inference

Phylogenetic relationships across the genome between species of *Melinaea* and *Mechanitis* were inferred using the multispecies coalescent (MSC) approach implemented in BPP v.4.6.2 (110), while accounting for incomplete lineage sorting. For each species, only the individual with the highest coverage was included. To minimise the effect of linked selection, loci were required to be at least 2 kb from annotated exons. Because the analysis assumes no intra-locus recombination and independence between loci, we selected loci of 300 bp and at least 2 kb from neighbouring loci. Sequence alignments were produced for all loci, masking repetitive elements annotated in the reference genome using RepeatMasker v4.1.5 (http://repeatmasker.org/). For each locus, individuals with more than 80% missing genotype calls were excluded from the alignment and only loci with all individuals passing filters were considered. Furthermore, sites with missing genotype calls were removed and loci with less than 30 bp passing filters were excluded. Heterozygous sites were assigned IUPAC codes. Loci were grouped into blocks of 100 loci. Species-tree estimation was then performed in BPP v.4.6.2 using the A01 analysis (species-tree inference assuming no gene flow). Inverse gamma priors (invGs) were applied both to the root age ($\tau 0$) and to effective population sizes (θ) – invG(3, 0.06) and invG(3, 0.04), respectively. Parameters were scaled assuming a mutation rate of $2.9 \times 10{-}9$ substitutions per site per generation and 4 generations per year.

The MCMC was run for 1,000,000 iterations after 50,000 iterations of burn-in, sampling every 10 iterations.

Demographic modelling

For the three highly introgressed species *Mel. idae, Mec. messenoides* and *Mec. nesaea, we ran* a multispecies-coalescent-with-introgression (MSCi) model implemented in BPP v.4.6. 2 (110) to better estimate their position in the phylogeny and divergence timing while accounting for admixture. For *Mel. idae* we considered *Mel. lilis* and *Mel. marsaeus* as sister/donor species, while for *Mec. messenoides*, *Mec. menapis* and *Mec. polymnia* (West) were chosen. For *Mec. nesaea*, we used one individual of each of the Brazilian populations (*Mec. nesaea, Mec. lysimnia lysimnia*, *Mec. polymnia casabranca*). Loci were selected randomly from autosomes, and required to be at least 2 kb from annotated exons and 10 kb from the nearest locus, and a maximum size of 2 kb. For each locus, individuals with more than 50% missing data and sites containing missing genotypes or overlapping annotated repetitive elements were removed. Only loci at least 800 bp long after filters and without missing individuals were considered. Heterozygous sites were assigned IUPAC codes. Demographic parameters were estimated using a fixed species tree with introgression events (Fig. S11). An inverse gamma prior (invG) was applied for all population size parameters θ (α=3; β=0.04) and root age parameter τ (α=3; β=0.06). A beta prior was applied to the introgression probability (ϕ) (α=1; β=1). Three replicate MCMC runs of 1,000,000 iterations, after a burn-in period of 50,000 iterations, sampling every 50 iterations were performed for each dataset. Divergence time was calculated based on 4 generations per year, and a mutation rate of 2.90E-09 as in *Heliconius* (43) ($T=\tau$/mutation rate/generations/million years).

Genome scans and ADMIXTURE

F_{ST}, D_{XY} and pi (π) were calculated in all species pairs in 20kb windows (including monomorphic sites, with a minimum of 10,000 sites per window) across the genome with the scripts from Simon Martin (https://github.com/simonhmartin/genomics_general). We also ran ADMIXTURE in subsets of *Mechanitis* and *Melinaea* to see clustering between individuals with k ranging from 2 to 9 (111). For this dataset, we used the same filter settings as for the Fbranch analysis (see above).

Introgression (f_{dM}) scans

To examine gene flow across the genome of *Mec. nesaea*, we computed f_{dM} with the script by Simon Martin (ABBABABAwindows.py, https://github.com/simonhmartin/genomics_general) (112) with various

549 populations for P1,2,3,4. If for example P1=*Mec. polymnia casabranca* (Brazil), P2=*Mec. nesaea*, P3=*Mec.*
550 *lysimnia* Brazil, and P4=*Forbestra*, high f_{dM} values indicate introgression between *Mec. lysimnia* and *Mec.*
551 *nesaea*. We also tested other outgroups (*Mec. messenoides*) and with five single *Mec. nesaea* individuals,
552 to see if the signal was consistent in different individuals (Fig. S14).
553
554 *Androconial Chemistry*
555 We obtained samples of the androconial secretions from 92 males (Text S5). To exclude non-androconial
556 compounds from our analyses, for each population the same extraction procedure was adopted with
557 wings of conspecific females and two non-androconial wing areas of males. Eight solvent negative controls
558 were also taken for each sampling event.
559 The peak areas of each chromatogram were integrated with MSD ChemStation E.02.01.1177
560 (Agilent Technologies, USA) to obtain the total ion current signals. A series of linear alkanes (C7–C40) was
561 used to determine the linear retention indices (RI) of each compound (113). Compounds were identified
562 by comparing their mass spectra and retention indices with those of reference samples available from
563 personal and commercial mass spectral libraries (FFNSC 2, MassFinder 4, NIST17, MACE v.5.1 (114), and
564 Wiley Registry™ 9th ed.). The peaks exclusive to the androconial samples were used to determine the
565 relative percentages of each compound per sample.
566 Dihydropyrrolizines, such as hydroxydanaidal or methyl hydroxydanaidoate, are typically
567 accompanied by smaller peaks formed by degradation during GC/MS analyses and/or storage (115). These
568 degradation peaks were excluded from the generated ion chromatograms and statistical analysis. To avoid
569 non-evident contaminants, we only considered compounds present in more than three individuals for any
570 given taxon.
571 The data were plotted in R (116) using the vegan package
572 (https://doi.org/10.32614/CRAN.package.vegan) for nonmetric multidimensional scaling with
573 'monoMDS', specifying a global model, square root transformation and Wisconsin double standardisation
574 (autotransform=TRUE).
575
576 *Chromosome rearrangements*
577 Synteny and breakpoint analysis was performed using single copy orthologous genes identified with
578 BUSCO version 5.7.1 with the lineage database lepidoptera_odb10 and otherwise default options (117).
579 To compare large scale rearrangements in the *Mechanitis* and *Melinaea* versus the butterfly ancestral
580 linkage groups (Merian elements), we used two outgroup genomes, *Melitaea cinxia* (118) and *Danaus*

plexippus (119). The output from BUSCO was filtered with a custom script to contain only complete genes located in chromosome-sized scaffolds and excluding W. Only single copy genes were included with the exception of genes on the neo-Z2*,* where we also included genes classified as duplicated. The sex linking of Z2 appears to be recent and most of the genes had high similarity to the genes on the corresponding W's and were therefore classified as duplicated by BUSCO. Genes that were actually duplicated (occurring more than once or present on other chromosomes than W) on the Z2 were removed. We determined syntenic blocks, excluding single gene translocations, by comparing the position of the BUSCO-genes in each genome against the Merian elements (*Melitaea cinxia*), and visualised the syntenic relationship with the R-package gggenomes (120). Minimum number of fusions were determined by the number of different Merian elements located in every query chromosome and fissions were determined as the number of query chromosomes containing parts of each Merian element for each species. The breakpoints between all species within *Mechanitis* and *Melinaea* was determined by the same principle as above using an all against all approach for each genome to compare the BUSCO-gene positions. Synteny analysis of the sex chromosomes and between haplotypes were performed with whole genome alignment using minimap2/2.27 with default settings and -x asm10 (1% sequence divergence) (121) and visualised after removing short alignments (<100kb for multispecies alignment, <500kb for haplotype alignment) using a modified version of the R-package Farre-lab/syntenyPlotteR (122).

To investigate the association between chromosomal rearrangements and species divergence we mapped the location of the breakpoints between each comparison to the reference genomes *Mec. messenoides* and *Mel. marsaeus*. Divergence and diversity was estimated in 20 kb windows along the genome (detailed above). To determine whether the observed statistics in the breakpoint regions were different from the random expectation of regions of the same size and number across the genome, we used permTest with the randomise function option 'randomizeRegions' and evaluate function option 'meanInRegions' for 50,000 permutations, as implemented in the R-package regioneR (123). The analyses above were performed in R v4.4.0 (116). For conservative interpretation multiple correction was performed with Bonferroni adjustment (α/n), where $\alpha = 0.05$ and $n = 10$ for the comparisons within each genus, resulting in values considered significantly different if their p-value from the randomisation test was less than 0.005.

Funding

This research was funded with the Wellcome Trust award 220540/Z/20/A, a Branco Weiss Fellowship, a Royal Society University Research Fellowship (URF\R1\221041) and a Bateson Research Fellowship by St

John's College, Cambridge awarded to JIM. ESMH was supported by NERC DTP C-CLEAR, the Zoology Department of the University of Cambridge, St John's College, Cambridge, and the Wellcome Sanger Institute PhD programme. CEBN had a PhD Scholarship from Coordenação de Aperfeiçoamento de Pessoal de Nível Superior. Sample collection was further supported by Leverhulme trust (KW and ME), a Phyllis and Eileen Gibbs Fellowship, ATIP grant, ANR SPECREP and CLEARWING, and HFSP RGP0014/2016 (ME and MM), a Research Fellowship from the Royal Commission for the Great Exhibition of 1851 and a Royal Society Research Grant (SHM) and Deutsche Forschungsgemeinschaft, Schu984/12-2 (SS).

Acknowledgements

We thank Ismael Aldas and Raúl Aldaz for assistance with catching butterflies in Ecuador, Mario Tuanama and Ronald Mori-Pezo for help with rearing and collecting butterflies in Peru, Augusto Rosa for sampling support in São Paulo, Erika de Castro for sampling in Brazil, Mathieu Joron for sampling in French Guiana and John R. MacDonald for sampling in Panama. We thank the Peruvian, Ecuadorian and Brazilian authorities as well as the Museo de Historia Natural in Peru and the Museo Ecuatoriano de Ciencias Naturales in Ecuador for their support. Many thanks to Dr Blanca Huertas and Robyn Crowther from the Natural History Museum in London (NHMUK) for providing butterfly legs of *Mel. isocomma* and *Mel. mothone* and to Dr Petra Korlevic for assistance with extracting DNA from museum specimens. We are grateful to the editor and reviewers for their helpful comments that have greatly improved our manuscript.

Data, materials and software availability

All code and tables underlying the figures are found in our GitHub repository: https://github.com/rapidspeciation/mechanitis_melinaea.

References

1. J. B. Losos, Adaptive radiation, ecological opportunity, and evolutionary determinism : American society of naturalists E. O. Wilson award address. *American Naturalist* **175**, 623–639 (2010).

2. R. G. Gillespie, *et al.*, Comparing Adaptive Radiations Across Space, Time, and Taxa in *Journal of Heredity*, (Oxford University Press, 2020), pp. 1–20.

3. E. Gittenberger, Radiation and adaptation, evolutionary biology and semantics. *organisms, diversity & evolution* **4**, 135–136 (2004).

4. J. E. Czekanski-Moir, R. J. Rundell, The Ecology of Nonecological Speciation and Nonadaptive Radiations. *Trends in Ecology & Evolution* **34**, 400–415 (2019).

5. R. De-Kayne, *et al.*, Why Do Some Lineages Radiate While Others Do Not? Perspectives for Future Research on Adaptive Radiations. *Cold Spring Harb Perspect Biol* a041448 (2024). https://doi.org/10.1101/cshperspect.a041448.

6. J. Cerca, *et al.*, Evolutionary genomics of oceanic island radiations. *Trends in Ecology & Evolution* **38**, 631–642 (2023).

7. S. Claramunt, Discovering exceptional diversifications at continental scales: the case of the endemic families of neotropical suboscine passerines. *Evolution* (2010). https://doi.org/10.1111/j.1558-5646.2010.00971.x.

8. R. Maestri, *et al.*, The ecology of a continental evolutionary radiation: Is the radiation of sigmodontine rodents adaptive? *Evolution* **71**, 610–632 (2017).

9. S. Tiatragul, A. Skeels, J. S. Keogh, Morphological evolution and niche conservatism across a continental radiation of Australian blindsnakes. *Evolution* **78**, 1854–1868 (2024).

10. M. Doré, *et al.*, Anthropogenic pressures coincide with Neotropical biodiversity hotspots in a flagship butterfly group. *Diversity and Distributions* **28**, 2912–2930 (2022).

11. N. Chazot, *et al.*, Renewed diversification following Miocene landscape turnover in a Neotropical butterfly radiation. *Global Ecology and Biogeography* **28**, 1118–1132 (2019).

12. G. W. Beccaloni, K. J. Gaston, Predicting the species richness of neotropical forest butterflies: Ithomiinae (Lepidoptera: Nymphalidae) as indicators. *Biological Conservation* **71**, 77–86 (1995).

13. K. S. Brown, “Conservation of Neotropical Environments: Insects as Indicators” in *The Conservation of Insects and Their Habitats*, (Elsevier, 1991), pp. 349–404.

14. K. S. Brown, Adult-obtained pyrrolizidine alkaloids defend ithomiine butterflies against a spider predator. *Nature* **309**, 707–709 (1984).

15. P. J. Devries, F. G. Stiles, Attraction of Pyrrolizidine Alkaloid Seeking Lepidoptera to Epidendrum paniculatum Orchids. **22**, 290–297 (1990).

16. J. R. Trigo, K. S. Brown, Variation of pyrrolizidine alkaloids in Ithomiinae: a comparative study between species feeding on Apocynaceae and Solanaceae. *Chemoecology* **22**, 22–29 (1990).

17. A. V. L. Freitas, *et al.*, Tropane and pyrrolizidine alkaloids in the ithomiinesPlacidula euryanassa andMiraleria cymothoe (Lepidoptera: Nymphalidae). *Chemoecology* **7**, 61–67 (1996).

18. M. McClure, *et al.*, Why has transparency evolved in aposematic butterflies? Insights from the largest radiation of aposematic butterflies, the Ithomiini. *Proceedings of the Royal Society B: Biological Sciences* **286** (2019).

19. F. Müller, Ituna and Thyridia: a remarkable case of Mimicry in Butterflies. *Kosmos* **May**, 100 (1879).

20. G. W. Beccaloni, Ecology, natural history and behaviour of ithomiine butterflies and their mimics in Ecuador (Lepidoptera: Nymphalidae: Ithomiinae). *Tropical Lepidoptera* **8**, 103–124 (1997).

21. A. Y. Kawahara, *et al.*, A global phylogeny of butterflies reveals their evolutionary history, ancestral hosts and biogeographic origins. *Nature Ecology and Evolution* **7**, 903–913 (2023).

22. R. M. Fox, A monograph of the Ithomiidae (Lepidoptera). Part III. The Tribe Mechanitini. *Memoirs of the American Entomological Society* **22** (1967).

23. K. K. Dasmahapatra, M. Elias, R. I. Hill, J. I. Hoffman, J. Mallet, Mitochondrial DNA barcoding detects some species that are real, and some that are not. *Molecular Ecology Resources* **10**, 264–273 (2010).

24. M. Elias, *et al.*, Limited performance of DNA barcoding in a diverse community of tropical butterflies. *Proc. R. Soc. B.* **274**, 2881–2889 (2007).

25. R. I. Hill, *et al.*, Ecologically relevant cryptic species in the highly polymorphic Amazonian butterfly Mechanitis mazaeus s.l. (Lepidoptera: Nymphalidae; Ithomiini). *Biological Journal of the Linnean Society* **106**, 540–560 (2012).

26. K. S. Brown, Geographical patterns of evolution in Neotropical Lepidoptera: differentiation of the species of Melinaea and Mechanitis (Nymphalidae, Ithomiinae). *Systematic Entomology* **2**, 161–197 (1977).

27. W. T. M. Forbes, A second review of Melinaea and Mechanitis (Lepidoptera, Ithomiinae). *Journal of the New York Entomological Society* **56**, 1–24 (1948).

28. R. M. Fox, A monograph of the Ithomiidae (Lepidoptera). Part II. The Tribe Melinaeini Clark. *Transactions of the American Entomological Society* **86**, 109–171 (1960).

29. G. Lamas, Checklist: Part 4A. Hesperioidea - Papilionoidea. *Atlas of Neotropical Lepidoptera* **5** (2004).

30. K. R. Willmott, J. Mallet, Correlations between adult mimicry and larval host plants in ithomiine butterflies. *Proceedings of the Royal Society B: Biological Sciences* **271** (2004).

31. N. Chazot, *et al.*, Mutualistic Mimicry and Filtering by Altitude Shape the Structure of Andean Butterfly Communities. *The American Naturalist* **183**, 26–39 (2014).

32. M. McClure, M. Elias, Unravelling the role of host plant expansion in the diversification of a Neotropical butterfly genus. *BMC Evolutionary Biology* **16** (2016).

33. I. Birskis-Barros, A. V. L. Freitas, P. R. Guimarães, Habitat generalist species constrain the diversity of mimicry rings in heterogeneous habitats. *Sci Rep* **11**, 5072 (2021).

34. K. S. Brown, Quaternary refugia in tropical America: evidence from race formation in *Heliconius* butterflies. *Proc. R. Soc. Lond. B.* **187**, 369–378 (1974).

35. A. Whinnett, *et al.*, Strikingly variable divergence times inferred across an Amazonian butterfly 'suture zone.' *Proc. R. Soc. B.* **272**, 2525–2533 (2005).

36. K. K. Dasmahapatra, G. Lamas, F. Simpson, J. Mallet, The anatomy of a "suture zone" in Amazonian butterflies: A coalescent-based test for vicariant geographic divergence and speciation. *Molecular Ecology* **19**, 4283–4301 (2010).

37. J. Haffer, Speciation in Amazonian Forest Birds: Most species probably originated in forest refuges during dry climatic periods. *Science* **165**, 131–137 (1969).

38. N. Chazot, *et al.*, Contrasting patterns of Andean diversification among three diverse clades of Neotropical clearwing butterflies. *Ecology and Evolution* **8**, 3965–3982 (2018).

39. J. Mallet, Hybrid speciation. *Nature* **446**, 279–283 (2007).

40. The Heliconius Genome Consortium, Butterfly genome reveals promiscuous exchange of mimicry adaptations among species. *Nature* **487**, 94–98 (2012).

41. R. Abbott, *et al.*, Hybridization and speciation. *J of Evolutionary Biology* **26**, 229–246 (2013).

42. D. A. Marques, K. Lucek, V. C. Sousa, L. Excoffier, O. Seehausen, Admixture between old lineages facilitated contemporary ecological speciation in Lake Constance stickleback. *Nature Communications* **10** (2019).

43. N. Rosser, *et al.*, Hybrid speciation driven by multilocus introgression of ecological traits. *Nature* **628**, 811–817 (2024).

44. M. Barrier, B. G. Baldwin, R. H. Robichaux, M. D. Purugganan, Interspecific hybrid ancestry of a plant adaptive radiation: allopolyploidy of the Hawaiian silversword alliance (Asteraceae) inferred from floral homeotic gene duplications. *Molecular Biology and Evolution* **16**, 1105–1113 (1999).

45. J. I. Meier, *et al.*, Cycles of fusion and fission enabled rapid parallel adaptive radiations in African cichlids. *Science* **381**, eade2833 (2023).

46. R. W. R. Wallbank, *et al.*, Evolutionary Novelty in a Butterfly Wing Pattern through Enhancer Shuffling. *PLoS Biology* **14** (2016).

47. L. H. Rieseberg, *et al.*, Major Ecological Transitions in Wild Sunflowers Facilitated by Hybridization. *Science* **301**, 1211–1216 (2003).

48. K. S. Brown, B. V. Schoultz, E. Suomalainen, Chromosome evolution in Neotropical Danainae and Ithomiinae (Lepidoptera). *Hereditas* **141**, 216–236 (2004).

49. C. A. Everett, J. B. Searle, B. M. N. Wallace, A study of meiotic pairing, nondisjunction and germ cell death in laboratory mice carrying Robertsonian translocations. *Genet. Res.* **67**, 239–247 (1996).

50. F. J. Ayala, M. Coluzzi, Chromosome speciation: Humans, Drosophila, and mosquitoes. (2005).

51. K. Yoshida, *et al.*, Chromosome fusions repatterned recombination rate and facilitated reproductive isolation during Pristionchus nematode speciation. *Nat Ecol Evol* (2023). https://doi.org/10.1038/s41559-022-01980-z.

52. M. A. F. Noor, K. L. Grams, L. A. Bertucci, J. Reiland, Chromosomal inversions and the reproductive isolation of species. *Proc. Natl. Acad. Sci. U.S.A.* **98**, 12084–12088 (2001).

53. L. H. Rieseberg, Chromosomal rearrangements and speciation. (2001).

54. M. McClure, B. Dutrillaux, A.-M. Dutrillaux, V. Lukhtanov, M. Elias, Heterozygosity and Chain Multivalents during Meiosis Illustrate Ongoing Evolution as a Result of Multiple Holokinetic Chromosome Fusions in the Genus *Melinaea* (Lepidoptera, Nymphalidae). *Cytogenet Genome Res* **153**, 213–222 (2017).

55. J. Mallet, A species definition for the Modern Synthesis. *TREE* **10**, 294–299 (1995).

56. M. McClure, M. Elias, Ecology, life history, and genetic differentiation in Neotropical Melinaea (Nymphalidae: Ithomiini) butterflies from north-eastern Peru. *Zoological Journal of the Linnean Society* **179**, 110–124 (2016).

57. A. H. B. Rosa, E. P. Barbosa, N. Wahlberg, A. V. L. Freitas, Systematic position and conservation aspects of Melinaea mnasias thera (Lepidoptera: Nymphalidae: Danainae). *Nat. Conserv. Res.* **9** (2024).

58. J. Vasconcellos-Neto, K. S. Brown, Interspecific Hybridization in Mechanitis Butterflies (Ithomiinae): a Novel Pathway for the Breakdown of Isolating Mechanisms. *Biotropica* **14**, 288 (1982).

59. R. Robinson, *Lepidoptera Genetics* (Pergamon, 1971).

60. J. Gauthier, *et al.*, First chromosome scale genomes of ithomiine butterflies (Nymphalidae: Ithomiini): Comparative models for mimicry genetic studies. *Molecular Ecology Resources* **23**, 872–885 (2023).

61. S. H. Martin, J. W. Davey, C. Salazar, C. D. Jiggins, Recombination rate variation shapes barriers to introgression across butterfly genomes. *PLoS Biol* **17**, e2006288 (2019).

62. K. Näsvall, *et al.*, Nascent evolution of recombination rate differences as a consequence of chromosomal rearrangements. *PLoS Genet* **19**, e1010717 (2023).

63. T. E. Cruickshank, M. W. Hahn, Reanalysis suggests that genomic islands of speciation are due to reduced diversity, not reduced gene flow. *Molecular Ecology* **23**, 3133–3157 (2014).

64. K. M. Kozak, *et al.*, Multilocus species trees show the recent adaptive radiation of the mimetic heliconius butterflies. *Systematic Biology* **64**, 505–524 (2015).

65. M. Rossi, *et al.*, Adaptive introgression of a visual preference gene. (2024).

66. M. Kirkpatrick, N. Barton, Chromosome Inversions, Local Adaptation and Speciation. *Genetics* **173**, 419–434 (2006).

67. A. Mackintosh, Chromosome Fissions and Fusions Act as Barriers to Gene Flow between Brenthis Fritillary Butterflies. *Molecular Biology and Evolution* **40** (2023).

68. C. J. Wright, L. Stevens, A. Mackintosh, M. Lawniczak, M. Blaxter, Comparative genomics reveals the dynamics of chromosome evolution in Lepidoptera. *Nat Ecol Evol* **8**, 777–790 (2024).

69. V. A. Lukhtanov, V. Dincă, G. Talavera, R. Vila, Unprecedented within-species chromosome number cline in the Wood White butterfly Leptidea sinapis and its significance for karyotype evolution and speciation. *BMC Evol Biol* **11**, 109 (2011).

70. H. Augustijnen, *et al.*, A macroevolutionary role for chromosomal fusion and fission in Erebia butterflies. *Science Advances* (2024).

71. J. M. De Vos, H. Augustijnen, L. Bätscher, K. Lucek, Speciation through chromosomal fusion and fission in Lepidoptera. *Phil. Trans. R. Soc. B* **375**, 20190539 (2020).

72. L. Höök, K. Näsvall, R. Vila, C. Wiklund, N. Backström, High-density linkage maps and chromosome level genome assemblies unveil direction and frequency of extensive structural rearrangements in wood white butterflies (Leptidea spp.). *Chromosome Res* **31**, 2 (2023).

73. V. A. Lukhtanov, *et al.*, Versatility of multivalent orientation, inverted meiosis, and rescued fitness in holocentric chromosomal hybrids. *Proc. Natl. Acad. Sci. U.S.A.* **115** (2018).

74. S. Garagna, M. Zuccotti, J. B. Searle, C. A. Redi, P. J. Wilkinson, Spermatogenesis in heterozygotes for Robertsonian chromosomal rearrangements from natural populations of the common shrew, Sorex araneus. *Reproduction* **87**, 431–438 (1989).

75. S. Potter, *et al.*, Limited Introgression between Rock-Wallabies with Extensive Chromosomal Rearrangements. *Molecular Biology and Evolution* **39**, msab333 (2022).

76. J. B. S. Haldane, Sex ratio and unisexual sterility in hybrid animals. *Journ. of Gen.* **12**, 101–109 (1922).

77. L. Z. Carabajal Paladino, *et al.*, Sex Chromosome Turnover in Moths of the Diverse Superfamily Gelechioidea. *Genome Biology and Evolution* **11**, 1307–1319 (2019).

78. A. J. Mongue, M. E. Hansen, J. R. Walters, Support for faster and more adaptive Z chromosome evolution in two divergent lepidopteran lineages*. *Evolution* **76**, 332–345 (2022).

79. D. Charlesworth, B. Charlesworth, Sex differences in fitness and selection for centric fusions between sex-chromosomes and autosomes. *Genet. Res.* **35**, 205–214 (1980).

80. N. Rueda-M, *et al.*, Genomic evidence reveals three W-autosome fusions in Heliconius butterflies. *PLoS Genet* **20**, e1011318 (2024).

81. J. Šíchová, *et al.*, Fissions, fusions, and translocations shaped the karyotype and multiple sex chromosome constitution of the northeast-Asian wood white butterfly, *Leptidea amurensis*. *Biol. J. Linn. Soc.* **118**, 457–471 (2016).

82. T. Xiong, *et al.*, A polygenic explanation for Haldane's rule in butterflies. *Proc. Natl. Acad. Sci. U.S.A.* **120**, e2300959120 (2023).

83. J. April, R. H. Hanner, A.-M. Dion-Côté, L. Bernatchez, Glacial cycles as an allopatric speciation pump in north-eastern American freshwater fishes. *Molecular Ecology* **22**, 409–422 (2013).

84. B. Nevado, N. Contreras-Ortiz, C. Hughes, D. A. Filatov, Pleistocene glacial cycles drive isolation, gene flow and speciation in the high-elevation Andes. *New Phytologist* **219**, 779–793 (2018).

85. P. M. B. Bacquet, *et al.*, Selection on male sex pheromone composition contributes to butterfly reproductive isolation. *Proc. R. Soc. B.* **282**, 20142734 (2015).

86. R. M. Merrill, *et al.*, The diversification of Heliconius butterflies: What have we learned in 150 years? *Journal of Evolutionary Biology* **28**, 1417–1438 (2015).

87. T. H. Q. Powell, *et al.*, The Build-Up of Population Genetic Divergence along the Speciation Continuum during a Recent Adaptive Radiation of Rhagoletis Flies. *Genes* **13**, 275 (2022).

88. M. Kucka, Chan, Yingguang Frank, HMW DNA extraction using magnetic beads. *protocols.io* (2022). https://dx.doi.org/10.17504/protocols.io.b46bqzan.

89. P. Korlević, *et al.*, A Minimally Morphologically Destructive Approach for DNA Retrieval and Whole-Genome Shotgun Sequencing of Pinned Historic Dipteran Vector Species. *Genome Biology and Evolution* **13**, evab226 (2021).

90. S. Picelli, *et al.*, Tn5 transposase and tagmentation procedures for massively scaled sequencing projects. *Genome Research* **24**, 2033–2040 (2014).

91. Andrews, S, FastQC: A quality control tool for high throughput sequence data. (2010).

92. S. Chen, Y. Zhou, Y. Chen, J. Gu, Fastp: An ultra-fast all-in-one FASTQ preprocessor in *Bioinformatics*, (Oxford University Press, 2018), pp. i884–i890.

93. H. Li, R. Durbin, Fast and accurate short read alignment with Burrows-Wheeler transform. *Bioinformatics* **25**, 1754–1760 (2009).

94. Picard, Picard Toolkit. *Broad Institute* (2019). https://broadinstitute.github.io/picard/.

95. P. Danecek, *et al.*, Twelve years of SAMtools and BCFtools. *GigaScience* **10** (2021).

96. A. McKenna, *et al.*, The genome analysis toolkit: A MapReduce framework for analyzing next-generation DNA sequencing data. *Genome Research* **20**, 1297–1303 (2010).

97. V. Ruano-Rubio, *et al.*, Scaling accurate genetic variant discovery to tens of thousands of samples. (2017). https://doi.org/10.1101/201178.

98. P. Danecek, *et al.*, The variant call format and VCFtools. *Bioinformatics* **27**, 2156–2158 (2011).

99. S. Purcell, *et al.*, PLINK: A tool set for whole-genome association and population-based linkage analyses. *American Journal of Human Genetics* **81**, 559–575 (2007).

100. B. Q. Minh, *et al.*, IQ-TREE 2: New Models and Efficient Methods for Phylogenetic Inference in the Genomic Era. *Molecular Biology and Evolution* **37**, 1530–1534 (2020).

101. D. T. Hoang, *et al.*, UFBoot2: Improving the Ultrafast Bootstrap Approximation. *Mol. Biol. Evol* **35**, 518–522 (2017).

102. H. A. Ogilvie, R. R. Bouckaert, A. J. Drummond, StarBEAST2 Brings Faster Species Tree Inference and Accurate Estimates of Substitution Rates. *Molecular Biology and Evolution* **34**, 2101–2114 (2017).

103. E. Pebesma, Simple Features for R: Standardized Support for Spatial Vector Data. *The R Journal* **10**, 439 (2018).

104. M. Tennekes, tmap: Thematic Maps in R. *J. Stat. Soft.* **84** (2018).

105. T. Appelhans, F. Detsch, C. Reudenbach, S. Woellauer, Mapview: Interactive viewing of spatial data in R. *R package* **version 2.11.2** (2023).

106. B. Q. Minh, M. W. Hahn, R. Lanfear, New methods to calculate concordance factors for phylogenomic datasets. *Molecular Biology and Evolution* **37**, 2727–2733 (2020).

107. M. Malinsky, M. Matschiner, H. Svardal, Dsuite - Fast D-statistics and related admixture evidence from VCF files. *Molecular Ecology Resources* **21**, 584–595 (2021).

108. R. Bouckaert, *et al.*, BEAST 2: A Software Platform for Bayesian Evolutionary Analysis. *PLoS Comput Biol* **10**, e1003537 (2014).

109. N. F. Müller, *et al.*, Joint inference of species histories and gene flow. [Preprint] (2018). Available at: http://biorxiv.org/lookup/doi/10.1101/348391 [Accessed 7 November 2024].

110. T. Flouri, X. Jiao, B. Rannala, Z. Yang, A Bayesian Implementation of the Multispecies Coalescent Model with Introgression for Phylogenomic Analysis. *Molecular Biology and Evolution* **37**, 1211–1223 (2020).

111. D. H. Alexander, J. Novembre, K. Lange, Fast model-based estimation of ancestry in unrelated individuals. *Genome Res.* **19**, 1655–1664 (2009).

112. S. H. Martin, J. W. Davey, C. D. Jiggins, Evaluating the Use of ABBA–BABA Statistics to Locate Introgressed Loci. *Molecular Biology and Evolution* **32**, 244–257 (2015).

113. H. van D. Dool, P. D. Kratz, A generalization of the retention index system including linear temperature programmed gas-liquid partition chromatography. *Journal of Chromatography A* **11**, 463–471 (1963).

114. S. Schulz, A. Möllerke, MACE – An Open Access Data Repository of Mass Spectra for Chemical Ecology. *J Chem Ecol* **48**, 589–597 (2022).

115. S. Schulz, *et al.*, Semiochemicals derived from pyrrolizidine alkaloids in male ithomiine butterflies (Lepidoptera: Nymphalidae: Ithomiinae). *Biochemical Systematics and Ecology* **32**, 699–713 (2004).

116. R Core Team, A language and environment for statistical computing. *R foundation for statistical computing* (2024). https://doi.org/10.1080/01621459.1972.10481279.

117. M. Manni, M. R. Berkeley, M. Seppey, F. A. Simão, E. M. Zdobnov, BUSCO Update: Novel and Streamlined Workflows along with Broader and Deeper Phylogenetic Coverage for Scoring of Eukaryotic, Prokaryotic, and Viral Genomes. *Molecular Biology and Evolution* **38**, 4647–4654 (2021).

118. R. Vila, *et al.*, The genome sequence of the Glanville fritillary, Melitaea cinxia (Linnaeus, 1758). *Wellcome Open Res* **6**, 266 (2021).

119. L. Gu, *et al.*, Dichotomy of Dosage Compensation along the Neo Z Chromosome of the Monarch Butterfly. *Current Biology* **29**, 4071-4077.e3 (2019).

120. T. Hackl, M. J. Ankenbrand, B. van Adrichem, gggenomes: a grammar of graphics for comparative genomics. *R package* (2024). https://github.com/thackl/gggenomes.

121. H. Li, Minimap2: pairwise alignment for nucleotide sequences. *Bioinformatics* **34**, 3094–3100 (2018).

122. S. Quigley, J. Damas, D. M. Larkin, M. Farré, syntenyPlotteR: a user-friendly R package to visualize genome synteny, ideal for both experienced and novice bioinformaticians. *Bioinformatics Advances* **3**, vbad161 (2023).

123. B. Gel, *et al.*, regioneR: an R/Bioconductor package for the association analysis of genomic regions based on permutation tests. *Bioinformatics* **32**, 289–291 (2016).

124. M. Carvalho, A. Victor, L. Freitas, E. Barbosa, Immature stages of Mechanitis polymnia casabranca (Nymphalidae, Danainae). (2019). https://doi.org/10.5281/zenodo.2650300.

125. D. H. A. Melo, A. V. L. Freitas, Immature stages of Mechanitis lysimnia nesaea (Nymphalidae: Danainae: Ithomiini). *Tropical Lepidoptera* **33**, 79–85 (2023).

923 **Figures**

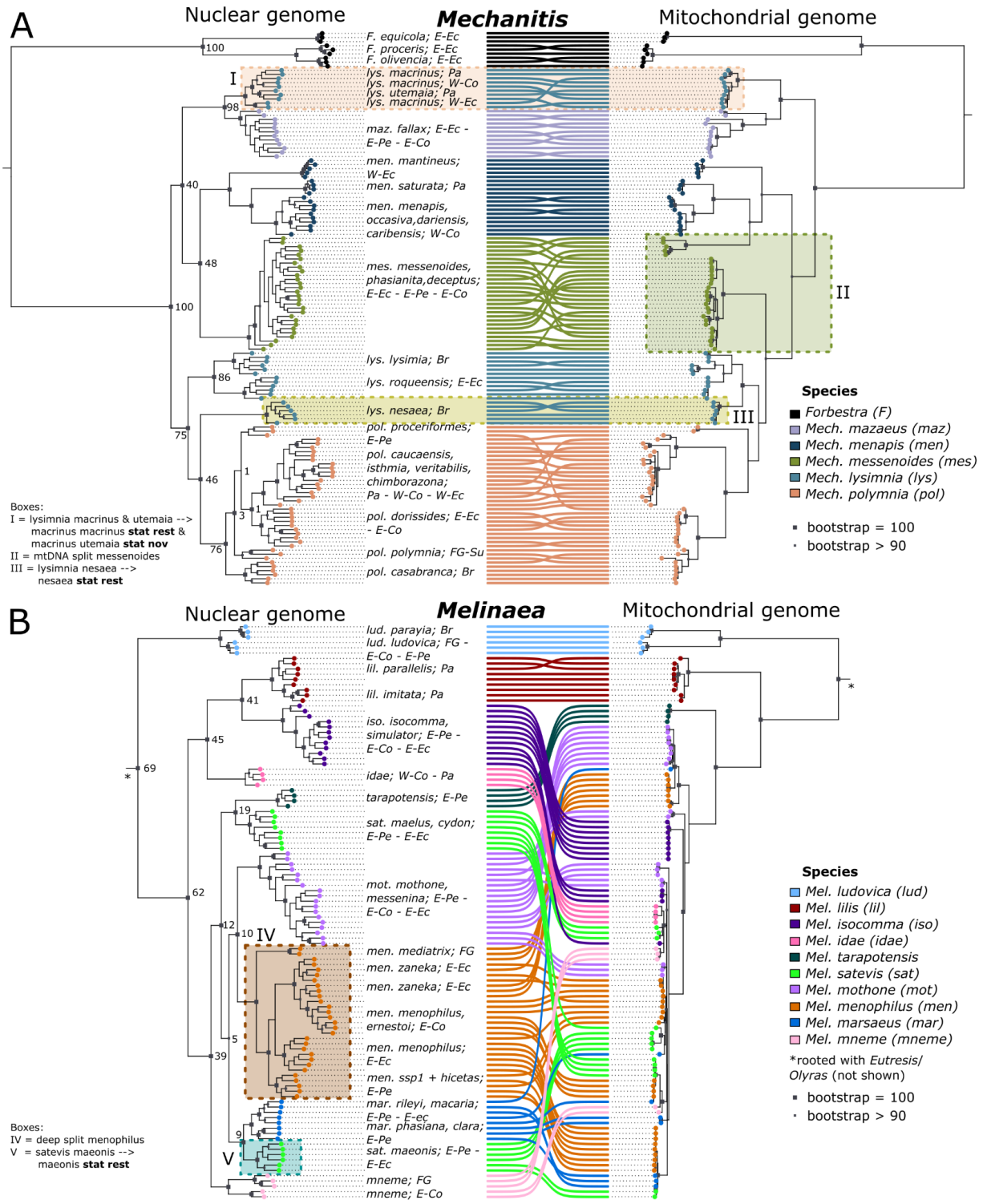

924

925 **Figure 1 - Rampant cytonuclear discordance in *Mechanitis and Melinaea* and a need for taxonomic revision**

Co-phyloplot showing the nuclear and mitochondrial phylogenies of 135 Mechanitis *and 109* Melinaea *individuals. Nuclear phylogeny (left) based on 537,500 SNPs for* Mechanitis ***(A)*** *and 784,526 SNPs for* Melinaea ***(B)*** *and full mitochondrial genome phylogeny (right). The coloured circles and connecting lines indicate the currently classified species* (25, 29)*. Br=Brazil; FG=French Guiana; E-Co=eastern Colombia; W-Co=western Colombia; E-Ec=eastern Ecuador; W-Ec=western Ecuador; E-Pe=eastern Peru; Pa=Panama, Su=Suriname. The coloured boxes highlight key findings. The node labels show concordance factors, indicating the percentage of trees produced for windows across the genome that contain that clade.*

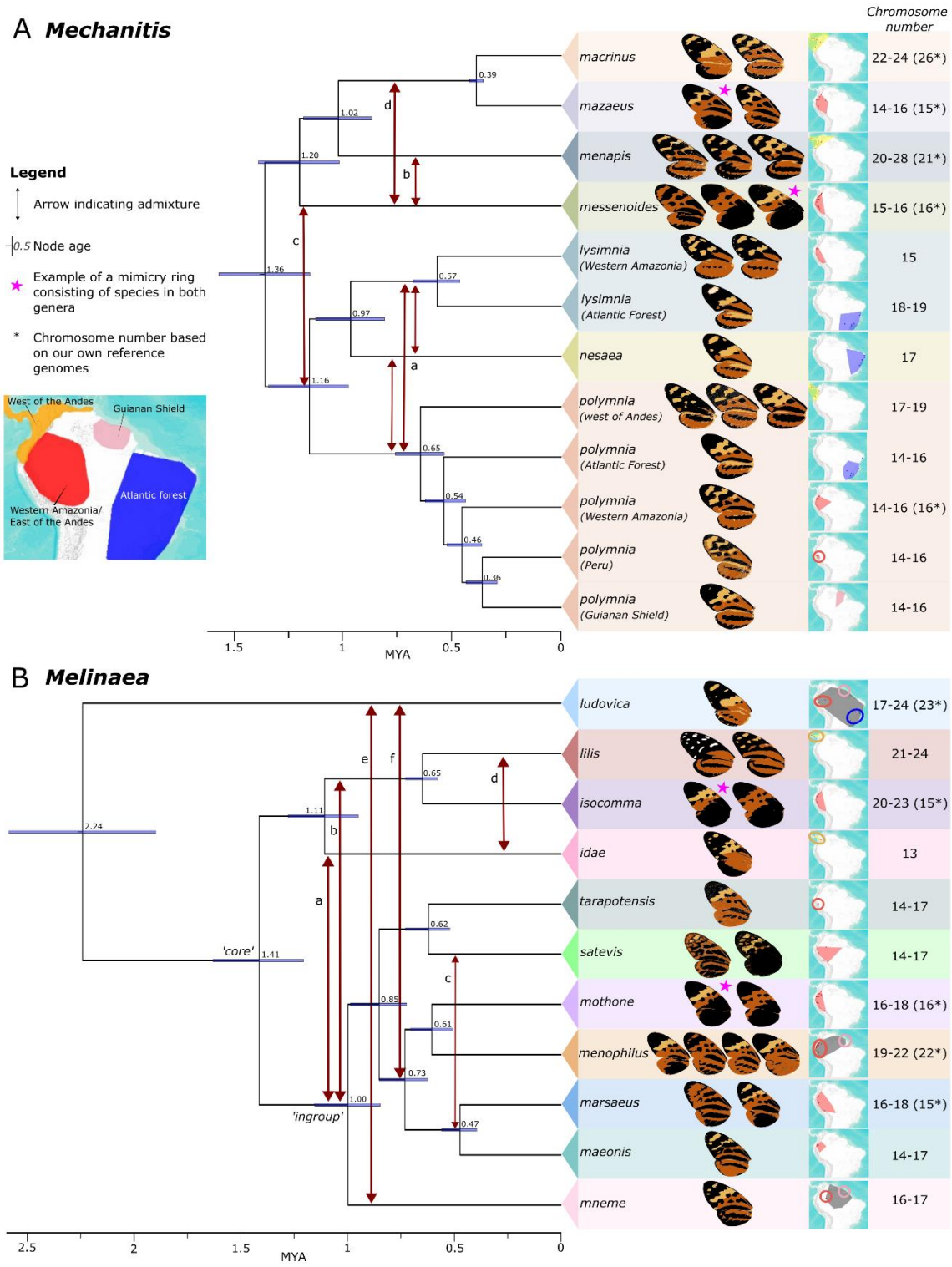

Figure 2 - Calibrated phylogeny of *Mechanitis and Melinaea* butterflies with evidence of introgression and biogeographic patterns.

Time-calibrated StarBEAST2 phylogenies of Mechanitis ***(A)*** *and* Melinaea ***(B)*** *with the newly proposed species classification and secondary calibrations from* (11)*. One individual was included at the species level, or subspecies-level if they were very divergent. The regions in the overview map are based on the combined distribution of our subspecies and samples from* (10) *with region names adapted from* (11)*. Arrows between clades indicate potential hybridisation events (based on AIM, Fbranch and BPP). The node labels indicate the age as obtained by the calibration. 'Core' in the* Melinaea *phylogeny indicates the core clade of fast diverging* Melinaea*, and 'ingroup' is a clade referred to in the text. For each clade, cartoon wings based on representative colour patterns are shown, and as an example, pink stars designate taxa part of the same mimicry ring. The distribution of our individuals is indicated by coloured dots and coloured rings on a distribution map based on the subspecies distribution from* (10)*); map from USGS, Esri, TANA, DeLorme and NPS; see Fig. S6-7 for larger maps). The chromosome numbers in the right column are based on* (48) *or our reference genomes (asterisk).*

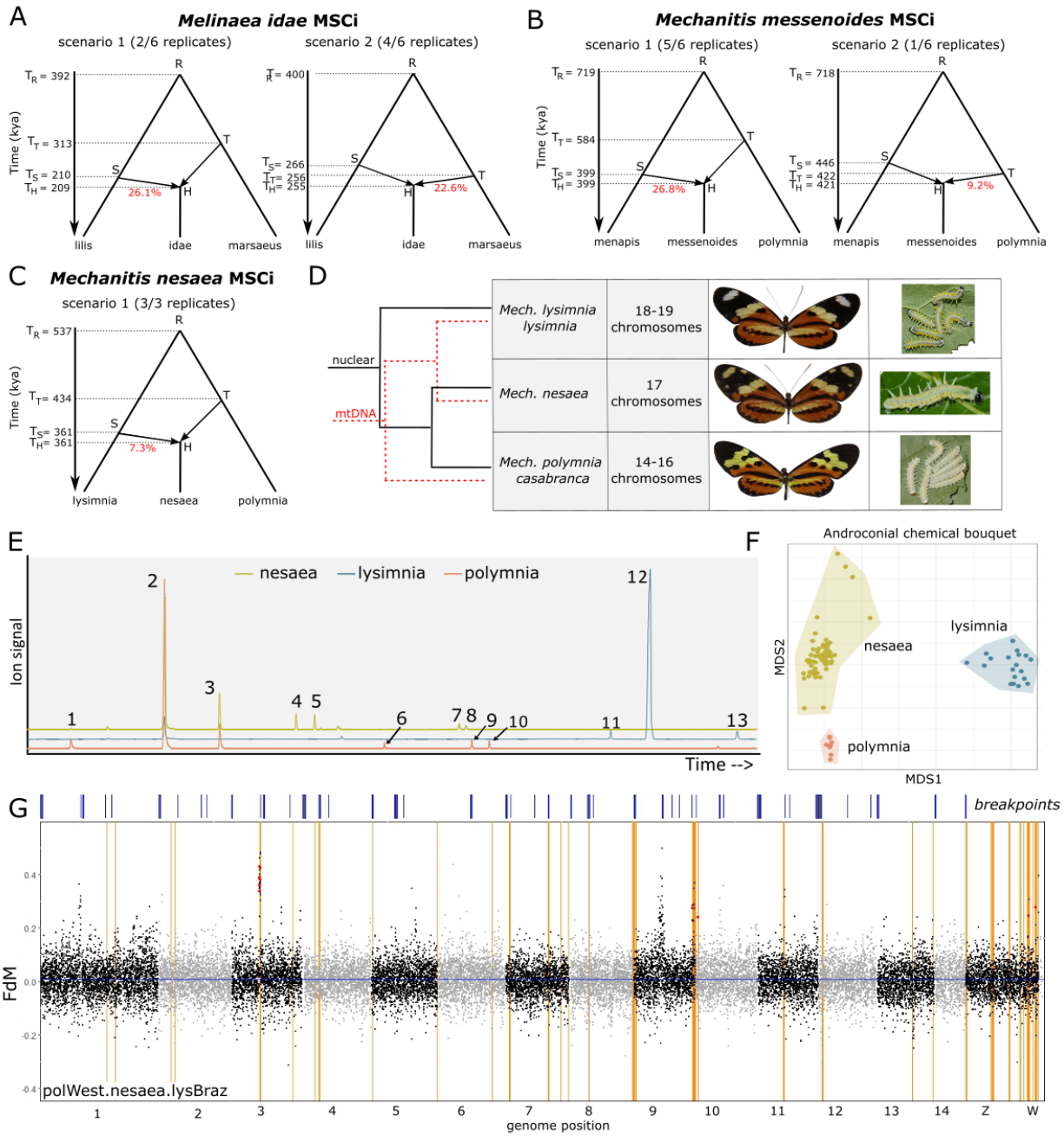

Figure 3 - *Three ancestrally introgressed species, with a focus on* Mechanitis nesaea

A multispecies coalescent-with-introgression model explored the relation and timing of introgression relative to the divergence times, in ***A)*** Mel. lilis*,* Mel. idae *and* Mel. marsaeus*;* ***B)*** Mec. menapis*,* Mec. messenoides*, and* Mec. polymnia*; and* ***C)*** *the Brazilian* Mec. lysimnia lysimnia, Mec. nesaea *and* Mec. polymnia casabranca. ***D)*** *A closer look into the restored species* Mec. nesaea*: phylogenetic relationships, chromosome numbers* (48)*, a photo of a representative adult and an early fifth instar larva* (124, 125)*. The photo of* M. lysimnia lysimia *is a courtesy of Augusto Rosa.* ***E)*** *Overlaid chromatograms of androconial extracts of representative individuals of* Mec. nesaea *(yellow line),* Mec. l. lysimnia *(blue) and* Mec. polymnia casabranca *(orange). Peaks: (1) 4-Hydroxy-3,5,5-*

trimethylcyclohex-2-enone, (2) Hydroxydanaidal, (3) Methyl hydroxydanaidoate, (4) Methyl farnesoate isomer, (5) Methyl (E,E)-farnesoate, (6) m/z *57, 43, 55, 56, 85, (7) Octadecatrienoic acid (cf.), (8) Octadecanoic acid, (9) Ethyl linolenate, (10)* (E)*-Phytyl acetate (11) Hexacosene, (12) Heptacosene, (13) Nonacosene (not all compounds of Table S3 are found in these three individuals).* ***F)*** *NMDS shows the androconial chemical bouquet of* Mec. nesaea *is clearly distinct from both putative parental lineages, most similar to* Mec. polymnia*.* ***G)*** *A genome scan of* f_{dM} *across the genome (in 20kb windows) reveals that strong signatures of introgression* (f_{dM}) *between* Mec. nesaea *and* Mec. lysimnia *(P1=allopatric polymnia,P2=nesaea,P3=lysimnia,P4=Forbestra) overlaps with regions of high differentiation* (F_{ST}) *between* Mec. nesaea *and its sister species* Mec. polymnia *(orange vertical lines - high* F_{ST}*, red dots - high* f_{dM} *and high* F_{ST}*). Chromosomal breakpoints between* Mec. polymnia *and the four other reference genomes are shown with blue bars on top.*

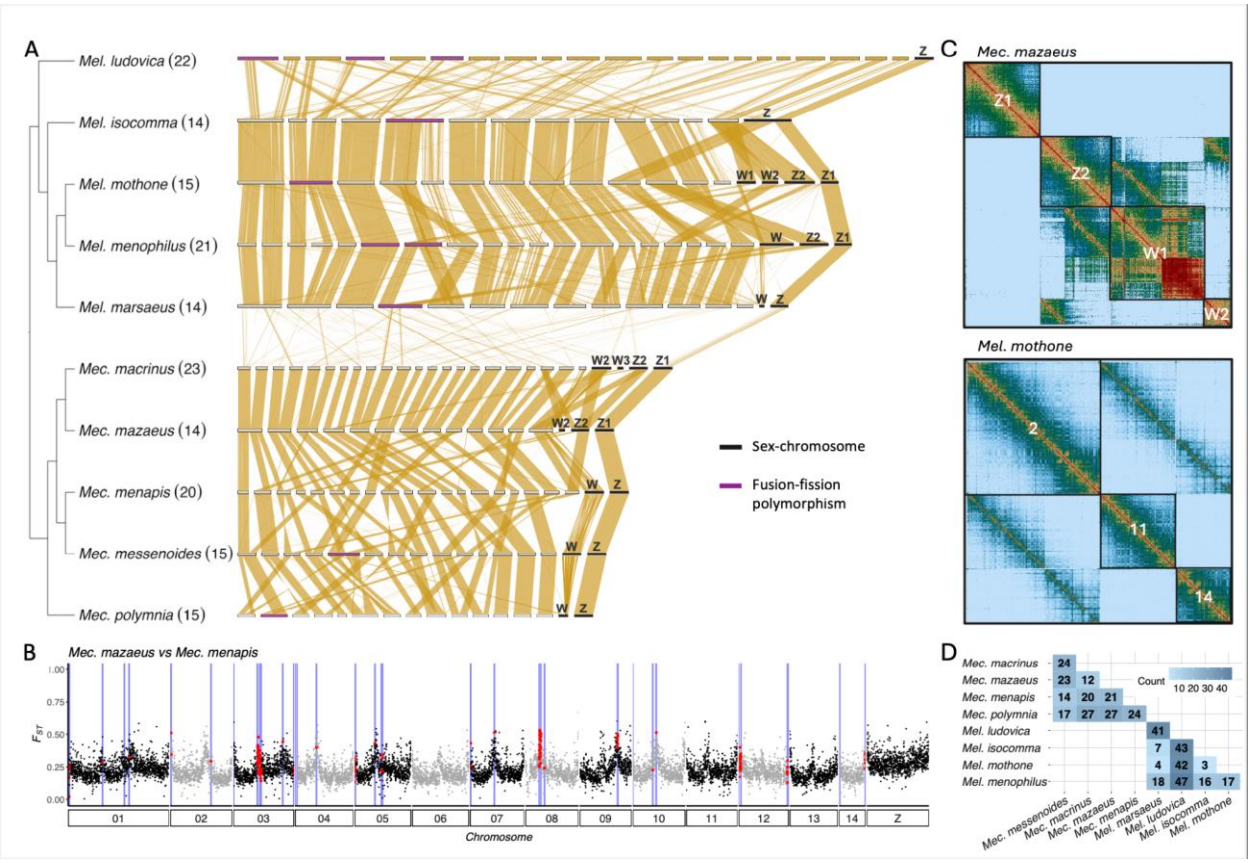

966

967 **Figure 4 - Chromosomal rearrangements**

968 ***A)*** *Synteny between* Melinaea *and* Mechanitis *genomes based on whole genome alignments. Horizontal bars*
969 *represent individual chromosomes, with sex-chromsomes (black bar) and chromosomes involved in within-species*
970 *polymorphic fusion-fissions (purple bar) highlighted. The cladogram is based on Fig. 2 and shows haploid*
971 *chromosome numbers in parentheses.* ***B)*** *Example of differentiation (F_{ST}) and breakpoints (blue vertical lines) between*
972 Mec. mazaeus *and* Mec. menapis along the genome*. The red dots indicate windows coinciding with breakpoints.* ***C)***
973 *Examples of HiC-contact maps. Top panel: Sex-chromosomes in* Mec. mazaeus*. Lower panel: Autosomal fission-fusion*
974 *heterozygote in* Mel. mothone*.* ***D)*** *Matrix displaying number of fusion-fission rearrangements between species in*
975 *each genus.*

976